

Supplementary material

### Triple-pyridyl iron complexes for in vivo photoacoustic imaging

Pan Xiang,<sup>‡ab</sup> Yu Shen,<sup>‡c</sup> JieShen,<sup>c</sup> Zhihui Feng,<sup>c</sup> Min Sun,<sup>a\*</sup> Qiong Zhang,<sup>c</sup> Shengli Li,<sup>c</sup> Dandan Li,<sup>c</sup> Guilong Zhang,<sup>c</sup> Zhengyan Wu,<sup>c</sup> YupengTian,<sup>c</sup> Zhongping Zhang,<sup>bd</sup> Xiaohe Tian<sup>ab\*</sup>

<sup>a</sup>*School of Life Science, Anhui University, Hefei 230601, P. R. China.*

<sup>b</sup>*Institute of Physical Science and Information Technology, Anhui University, Hefei 230601, P. R. China.*

<sup>c</sup>*Department of Chemistry, Anhui Province Key Laboratory of Chemistry for Inorganic/Organic Hybrid Functionalized Materials, Anhui University, Hefei 230601, P. R. China.*

<sup>d</sup>*CAS Center for Excellence in Nanoscience, Institute of Intelligent Machines, Chinese Academy of Sciences, Hefei 230000, P. R. China.*

<sup>e</sup>*Key Laboratory of High Magnetic Field and Ion Beam Physical Biology, Hefei Institutes of Physical Science, Chinese Academy of Sciences, Hefei 230031, P.R. China, zywu@ipp.ac.cn*

*E-mail address: [xiaohe.t@ahu.edu.cn](mailto:xiaohe.t@ahu.edu.cn), [sunmin@ahu.edu.cn](mailto:sunmin@ahu.edu.cn)*

*‡These authors contributed equally to this work and should be considered co-first authors.*

## Table of Content

Materials and apparatus.....	3
Synthetic procedures.....	3
Computational details.....	6
Oil-water partition coefficient experiment.....	6
Magnetic moment and molar susceptibility of <b>S-Fe</b> .....	7
Photothermal conversion efficiency test.....	7
PAI of <b>S-Fe</b> and <b>J-Fe</b> in phantom.....	8
Live cell and <i>ex vivo</i> experiment.....	8
Cell culture.....	8
Cytotoxicity assay.....	8
PAI of <b>S-Fe</b> <i>in vivo</i> .....	9
Scheme S1 Synthetic procedures for target molecules <b>S-Fe</b> , <b>J-Fe</b> and <b>O-Fe</b> .....	9
Figure S1. <sup>1</sup> H-NMR and <sup>13</sup> C-NMR spectra of <b>L2</b> , <b>S</b> and <b>O</b> .....	12
Figure S2. Mass spectra and <sup>1</sup> H-NMR spectra of <b>S-Fe</b> , <b>J-Fe</b> and <b>O-Fe</b> .....	17
Figure S3. Molecular orbital energy diagrams of (a) <b>O-Fe</b> , (b) <b>J-Fe</b> and (c) <b>S-Fe</b> .....	17
Figure S4. Oil-water partition coefficient of <b>S-Fe</b> , <b>J-Fe</b> and <b>O-Fe</b> .....	18
Figure S5. Ultraviolet absorption spectrum after incubation of <b>S-Fe</b> with 10% BSA.....	18
Figure S6. Rate of decay of TMB sensitized by <b>S-Fe</b> in PBS by the variation of the absorbance at 370 nm and 650 nm.....	19
Figure S7. a) 808 nm laser irradiation (0.5, 1.0 and 1.5 W cm <sup>-2</sup> ), heating curves of <b>S-Fe</b> and <b>J-Fe</b> aqueous solution. b) Photothermal conversion efficiency of <b>S-Fe</b> and <b>J-Fe</b> .....	19
Figure S8. Thermal stability of <b>S-Fe</b> (four cycles of laser on/off) under 808 nm laser (1 W cm <sup>-2</sup> ).19	
Table 1. Calculated linear absorption properties (nm), excitation energy (eV) and major contribution of <b>S-Fe</b> , <b>J-Fe</b> and <b>O-Fe</b> .....	20
Note and references.....	20

## Materials and apparatus

All chemicals and solvents were dried and purified by standard methods. The  $^1\text{H}$ -NMR spectra were obtained on Bruker AV 400 spectrometer (Germany) with TMS as internal standard. Mass spectra were performed on a Micromass GCT-MS spectrometer (UK). Magnetic susceptibilities were obtained by the Faraday method, at ambient temperature using a CAHN-200 magnetic balance setup, the apparatus being calibrated with  $\text{FeSO}_4 \cdot 7\text{H}_2\text{O}$ . UV-*vis* absorption spectra were recorded on a SHIMADZU UV-3600 spectrophotometer (Japan). Photoacoustic imaging was accomplished using an iThera medical in Vision 256-TF (German).

## Synthetic procedures

**Synthesis of L1:** The synthesis of **L1** was according to our previous work.<sup>1,2</sup>

**L1:**  $^1\text{H}$  NMR (600 MHz,  $\text{CDCl}_3$ )  $\delta$  (ppm) 9.83 (s, 1H), 7.7 (d, 2H), 7.4 (m, 4H), 7.14 (m, 6H), 7.0 (d, 2H);  $^{13}\text{C}$  NMR (150 MHz,  $\text{CDCl}_3$ )  $\delta$  (ppm) 190.46, 153.38, 146.17, 131.32, 129.75, 129.13, 126.34, 125.13, 119.37.

**Synthesis of L2:** **L1** (4.09 g, 0.015 mol) was dissolved in 20 mL of  $\text{CH}_2\text{Cl}_2$  in a three-necked flask, and stirred for 15 min at 0 °C. Then, chlorosulfonic acid (14.0 g, 0.12 mol) diluting with 30 mL of  $\text{CH}_2\text{Cl}_2$  was slowly added dropwise using a constant pressure dropping funnel. The reaction was continued for two hours under the conditions. Finally, the reaction was quenched by slowly adding an appropriate amount of water, and the temperature was raised to 40 °C for 2 h. After cooling to room temperature, the reaction was adjusted the pH to 7-8 with 4 mol/L NaOH. After adding ethanol, the water was rotated by a rotary evaporator, and finally recrystallized from methanol, suction filtered, and dried under vacuum for 24 h, yellow solid was obtained (5.86 g, yield 81.9 %).  $^1\text{H}$  NMR (400 MHz,  $d_6$ -DMSO)  $\delta$  (ppm) 9.80 (s, 1H), 7.76 (d,  $J=8.7$  Hz, 2H), 7.62 (d,  $J=8.5$  Hz, 4H), 7.10 (d,  $J=8.5$  Hz, 4H), 6.99 (d,  $J=8.7$  Hz, 2H).  $^{13}\text{C}$  NMR (101 MHz,  $d_6$ -DMSO)  $\delta$  (ppm) 190.75, 152.39, 145.67, 144.87, 131.24, 129.25, 127.34, 124.96, 119.45. ESI-MS  $m/z$ : calcd for:  $(\text{M}-\text{Na})^+$ : 454.00, found: 453.99.

## Synthesis of L3 and TsO:

The synthesis of **L3** and **TsO** were according to our previous work.<sup>3-5</sup>

L3:  $^1\text{H}$ NMR  $\delta$  (ppm) 8.77 (t, 2H), 8.64 (t, 4H), 8.02 (t, 2H), 7.76 (d, 2H), 7.52 (t, 2H), 6.89(d, 2H), 4.85 (t, 2H), 3.59 (q, 8H).  $^{13}\text{C}$  NMR (100 MHz,  $d_6$ -DMSO)  $\delta$  (ppm) 155.91, 155.37, 152.09, 150.01, 149.19, 137.22, 123.61, 128.30, 121.38, 118.04, 112.73, 61.73, 58.90.

TsO:  $^1\text{H}$  NMR (400 MHz,  $\text{CDCl}_3$ )  $\delta$  (ppm) 1.15~1.17 (t,  $J = 7.0$  Hz, 3H), 2.41 (s, 3H), 3.43~3.51 (q,  $J = 7.0$  Hz, 2H), 3.53~3.67 (m, 10H), 4.11~4.14 (t,  $J = 7.0$  Hz, 2H), 7.30~7.32 (d,  $J = 7.4$  Hz, 2H), 7.75~7.77 (d,  $J = 7.6$ Hz, 2H).  $^{13}\text{C}$  NMR (75 MHz,  $\text{CDCl}_3$ )  $\delta$  (ppm) 144.91, 133.02, 129.91, 128.04, 70.78, 70.69, 70.53, 69.81, 69.33, 68.72, 66.71, 21.70, 15,17.

**Synthesis of S:** A 250 mL three-necked flask was charged with NaOH (2.40 g, 0.068 mol) aqueous solution and 2-acetylpyridine (3.03 g, 0.025 mol), warmed to 80 °C, and stirred for 30 min. **L1** (4.33 g, 0.01 mol) was dissolved in an appropriate amount of ethanol, added to the above reaction system, and stirred for 30 min. An appropriate amount of  $\text{NH}_3 \cdot \text{H}_2\text{O}$  was added dropwise to the constant pressure dropping funnel, and the reaction was continued for 6 h. Solids were observed to precipitate, and the solution was clarified and allowed to stand overnight. After suction filtration, it was rinsed three times with ethanol, and the solid was recrystallized from methanol, and the obtained solid was dried in a vacuum oven for 24 h, yellow solid was obtained (4.12 g, yield 60.1 %).  $^1\text{H}$  NMR (400 MHz,  $\text{D}_2\text{O}$ )  $\delta$  (ppm) 8.22–8.08 (m, 2H), 7.72–7.60 (m, 2H), 7.52–7.34 (m, 8H), 7.10–6.98 (m, 2H), 6.83–6.74 (m, 2H), 6.73–6.60 (m, 4H), 6.41–6.29 (m, 2H).  $^{13}\text{C}$  NMR (101 MHz,  $d_6$ -DMSO)  $\delta$  (ppm) 155.58, 155.03, 149.29, 148.79, 148.61, 146.67, 137.41, 129.72, 127.91, 124.82, 124.44, 123.86, 122.26, 120.88, 117.11. ESI-MS  $m/z$ : calcd for: (M-2Na)/2: 317.05, found: 317.04. Anal. Calc. for  $\text{C}_{33}\text{H}_{22}\text{N}_4\text{Na}_2\text{O}_6\text{S}_2$ : C, 58.23; H, 3.26; N, 8.23 %; Found: C, 57.98; H, 3.46; N, 8.01 %.

**Synthesis of J:** The synthesis of **J** was according to our previous work.<sup>6</sup>

**J:**  $^1\text{H}$  NMR (400 MHz,  $\text{D}_2\text{O}$ )  $\delta$  (ppm) 8.12 (t,  $J = 20.9$  Hz, 2H), 7.89 (d,  $J = 7.9$  Hz, 2H), 7.68 (t,  $J = 7.6$  Hz, 2H), 7.49 (s, 2H), 7.31–7.15 (m, 4H), 6.34 (d,  $J = 8.3$  Hz, 2H), 3.63 (dd,  $J = 26.1, 18.2$  Hz, 4H), 3.46–3.27 (m, 4H), 3.15 (s, 18H).  $^{13}\text{C}$  NMR (100 MHz,  $\text{D}_2\text{O}$ )  $\delta$  (ppm) 153.89, 153.79, 147.93, 147.56, 145.86, 138.00, 127.57, 125.23, 124.24, 121.95, 116.20, 112.08, 61.05, 53.50, 43.89.

**Synthesis of O:** NaH (1.20 g, 0.03 mol) was dissolved in 30 mL of DMF in a 250 mL bottom flask under ice bath in nitrogen atmosphere. **L3** (12.14 g, 0.005 mol) was dissolved in DMF and added dropwise to a 250 mL round bottom flask using a constant pressure dropping funnel and

stirred for 30 min. **TsO** (3.19 g, 0.01 mol) was dissolved in DMF, slowly added to the above mixture, and stirred at 75 °C for 24 h. It was washed with water several times until the aqueous phase was neutral, extracted with ethyl acetate, dried over anhydrous MgSO<sub>4</sub> for 12 h, filtered and evaporated. Column chromatography purification (V petroleum ether/V ethyl acetate = 5/1), drying in a vacuum oven for 24 h, golden yellow oily liquid was obtained (2.75g, yield 77.7%). <sup>1</sup>H NMR (400 MHz, CD<sub>3</sub>OCD<sub>3</sub>) δ (ppm) 8.78 (d, J=3.1 Hz, 2H), 8.77–8.68 (m, 4H), 7.97 (td, J=7.7, 1.7 Hz, 2H), 7.82 (dd, J=9.0, 3.0 Hz, 2H), 7.48–7.41 (m, 2H), 6.95 (d, J=8.8 Hz, 2H), 3.72–3.42 (m, 28H), 3.27 (d, J=1.6 Hz, 4H), 2.98 (s, 6H). <sup>13</sup>C NMR (101 MHz, Acetone) δ (ppm) 157.09, 156.71, 150.61, 150.11, 137.81, 128.67, 125.46, 124.85, 121.81, 117.65, 112.99, 72.71, 71.42, 71.31, 71.17, 69.31, 58.91, 51.72. ESI-MS: calculated for m/z 704.38, found: (M+H) 705.3839 (M+Na) 727.3657. Anal. Calc. for C<sub>39</sub>H<sub>52</sub>N<sub>4</sub>O<sub>8</sub>: C, 66.46; H, 7.44; N, 7.95%; Found: C, 65.14; H, 7.44; N, 8.16%.

**Synthesis of S-Fe: S** (0.6542 g, 0.001 mol) was dissolved in dry acetonitrile and add iron dichloride (0.0811 g, 0.0005 mol) dropwise at 80 °C. After reacting for two hours, the reaction was stopped and cooled to room temperature. A purple solid was obtained by suction filtration. The solid was then recrystallized from methanol, suction filtered, and the solid was placed in a vacuum oven and dried for 24 h, purple solid was obtained (0.5209 g, yield 65%). <sup>1</sup>H NMR (400 MHz, *d*<sub>6</sub>-DMSO) δ (ppm) 9.52 (4 H, s), 8.95 (d, J=7.9 Hz, 4 H), 8.38 (d, J=8.4 Hz, 4 H), 7.96 (t, J= 7.7 Hz, 4 H), 7.61 (d, J=8.5 Hz, 8 H), 7.29 (d, J=8.5 Hz, 4 H), 7.21 (d, J=5.3 Hz, 4 H), 7.17 – 6.74 (12 H, m). <sup>13</sup>C NMR (101 MHz, *d*<sub>6</sub>-DMSO) δ (ppm) 155.59, 155.04, 149.30, 148.63, 146.67, 146.24, 137.42, 130.27, 129.73, 127.92, 124.82, 124.45, 123.87, 122.27, 120.88. ESI-MS m/z: calcd for: (M-2Na)/2: 662.06, found: 662.06. Anal. Calc. for C<sub>66</sub>H<sub>44</sub>FeN<sub>8</sub>O<sub>12</sub>S<sub>4</sub>: C, 46.44; H, 2.60; N, 6.56%; Found: C, 46.39; H, 2.61; N, 6.56%.

**Synthesis of J-Fe and O-Fe:** The preparations of **J-Fe** and **O-Fe** were similar with **S-Fe**.

**J-Fe:** <sup>1</sup>H NMR (400 MHz, *d*<sub>6</sub>-DMSO) δ (ppm) 8.82 (d, J=5.4 Hz, 4 H), 8.78 (4 H, s), 8.75 (4 H, s), 8.18 (t, J=7.5 Hz, 4 H), 7.96 (d, J=8.6 Hz, 4 H), 7.73 – 7.53 (4 H, m), 7.05 (d, J=8.9 Hz, 4 H), 3.95 – 3.88 (8 H, m), 3.58 – 3.44 (8 H, m), 3.21 (36 H, s). <sup>13</sup>C NMR (101 MHz, *d*<sub>6</sub>-DMSO) δ (ppm) 155.55, 155.12, 149.31, 147.25, 137.41, 128.10, 126.12, 124.41, 120.84, 116.64, 113.30, 60.42,

52.68, 43.66. ESI-MS  $m/z$ : calcd for: (M-6PF<sub>6</sub>)/6: 174.76, found: 174.76. Anal. Calc. for C<sub>62</sub>H<sub>80</sub>F<sub>36</sub>FeN<sub>12</sub>P<sub>6</sub>: C, 35.70; H, 4.12; N, 8.09%; Found: C, 35.65; H, 4.19; N, 8.13%.

**O-Fe:** <sup>1</sup>H NMR (400 MHz, *d*<sub>6</sub>-DMSO)  $\delta$  (ppm) 9.54 (4 H, s), 9.05 (d, *J*=8.1 Hz, 4 H), 8.43 (d, *J*=8.84 Hz, 4 H), 8.02 (d, *J*=7.5 Hz, 4 H), 7.24 (4 H, s), 7.19 (d, *J*=6.6 Hz, 4 H), 7.08 (d, *J*=8.9 Hz, 4 H), 3.71 (8 H, s), 3.69 – 3.36 (56 H, m), 3.24 (d, *J*=6.0 Hz, 12 H). <sup>13</sup>C NMR (101 MHz, D<sub>2</sub>O)  $\delta$  (ppm) 155.69, 149.50, 148.43, 147.87, 141.13, 129.26, 127.27, 123.05, 121.76, 118.88, 117.42, 112.46, 72.39, 71.69, 70.55, 70.25, 70.08, 68.29, 61.01, 57.98, 50.63. ESI-MS  $m/z$ : calcd for: (M-2PF<sub>6</sub>)<sup>-</sup>/2: 732.34, found: 732.34. Anal. Calc. for C<sub>78</sub>H<sub>104</sub>F<sub>12</sub>FeN<sub>8</sub>O<sub>16</sub>P<sub>2</sub>: C, 53.37; H, 5.97; N, 6.38%; Found: C, 53.29; H, 5.99; N, 6.34%.

### Computational details

The calculations were carried out with the Gaussian 09 software package. The optimizations of the complex structures were performed using B3LYP density functional theory. On the basis of ground- and excited- state optimization, the TDDFT approach was applied to investigate the excited state electronic properties.<sup>7, 8</sup>

### Oil-water partition coefficient experiment

Complexes **S-Fe**, **J-Fe** and **O-Fe** (2 mg) were dissolved in 5 ml n-octanol, and after completely dissolved, 2 mL mother liquor and 2 mL deionized water were separately mixed. The mixed solution was placed on a shaker for 12 h, then centrifuged at 4000 r/min for 15 min, and the supernatant and bottom were taken separately. 20  $\mu$ L of each liquid was placed in a centrifuge tube, 2 mL of n-octanol was added to the centrifuge tube containing the supernatant, 2 mL of deionized water was added to the centrifuge tube containing the bottom solution, and the absorbance was tested after mixing. Calculate its oil-water partition coefficient according to the following formula.

$\text{LogP} = \text{Lg } C_1/C_2$  ( $C_1$  represents the absorbance of the sample in n-octanol, and  $C_2$  represents the absorbance of the sample in deionized water).

### Magnetic moment and molar susceptibility of S-Fe

The magnetic moment and unpaired electron number were measured by Gouy magnetic balance method, and the permanent magnetic moment and unpaired electron number were obtained. The magnetic moment and unpaired electron number were calculated by the following equation:

$$X_m = \frac{2(\Delta m_{empty+sample} - \Delta m_{empty})ghM}{\mu_0 m H^2} (m^3 \cdot g^{-1})$$

$$X_m = X_{paramagn\&m} = \frac{N_A \mu_m^2 \mu_0}{3KT} (m^3 \cdot mol^{-1})$$

$$\mu_m = \mu_B \sqrt{n(n+2)}$$

$X_m$ : molar susceptibility.  $\Delta m_{empty+sample}$ : the weighing difference between after and before the magnetic field is applied to the sample tube (g).  $\Delta m_{empty}$ : the weighing difference between before and after the magnetic field is applied to the empty sample control.  $g$ : gravity acceleration ( $9.80 \text{ m} \cdot \text{s}^{-2}$ ).  $h$ : sample height (m).  $M$ : the molar mass of the sample ( $\text{g} \cdot \text{mol}^{-1}$ ).  $\mu_0$ : vacuum permeability ( $= 4\pi \times 10^{-7} \text{ kg} \cdot \text{m} \cdot \text{s}^{-1} \cdot \text{A}^{-2}$ ).  $m$ : mass of the sample (g).  $H$ : magnetic field intensity at the center of the magnetic pole ( $\text{A} \cdot \text{m}^{-1}$ ).  $N_A$ : Avogadro constant.  $\mu_m$ : molecular permanent magnetic moment.  $K$ : Boltzmann constant ( $1.38 \times 10^{-23} \text{ J} \cdot \text{K}^{-1}$ ).  $T$ : thermodynamic temperature.  $\mu_B$ : Bohr magneton ( $9.273 \times 10^{-24} \text{ J} \cdot \text{T}^{-1}$ ). So, molar susceptibility of S-Fe is  $-6.663 \times 10^9$ , the results show that the **S-Fe** is a diamagnetic metal complex, which indicates that the central ion Fe (II)  $d^6$  electron in the series of iron complexes is octahedral field with low spin.

### Photothermal conversion efficiency test

The aqueous solution of **S-Fe** (1.0 mL) in a quartz cell with different concentrations (0.1 mM, 0.5 mM and 1.0 mM) were exposed to laser irradiation (808 nm,  $1.0 \text{ W} \cdot \text{cm}^{-2}$ , 600 s), and water exposed to laser irradiation was used as a control sample. An IR-thermal camera was utilized to record the temperature of solutions every 60 s and the thermal images were also monitored and collected during irradiation. The photothermal conversion efficiency ( $\eta$ ) of the **S-Fe** was calculated according to the reported method.<sup>9</sup> Under continuous laser irradiation, the temperature of the **S-Fe** aqueous solution was recorded, until the solution had reached a steady-state temperature.

### PAI of S-Fe and J-Fe in phantom

Different concentrations of **S-Fe** and **J-Fe** were prepared with PBS, each of which was taken at 200  $\mu$ L in a 3.3 mm pipette and scanned separately by multispectral optical tomography system (MSOT in Vision 256, iThera Medical, Germany). Photoacoustic signals were detected under different excitation wavelengths (660-900 nm).

### **Live cell and *ex vivo* experiment**

#### **Cell culture**

HeLa cells purchased from Shanghai Bioleaf Bio Biotech. Co. Ltd. The cells were incubated in Dulbecco's Modified Eagle's medium (DMEM) containing 10% FBS and 1% antibiotics (penicillin and streptomycin), maintained at 37 °C in an atmosphere of 5% CO<sub>2</sub> and 95% air. Cells were seeded in 35 mm glass bottom cell culture dishes, at a density of  $1 \times 10^5$  cells and were allowed to grow when the cells reached more than 60% confluence.

#### **Cytotoxicity assay**

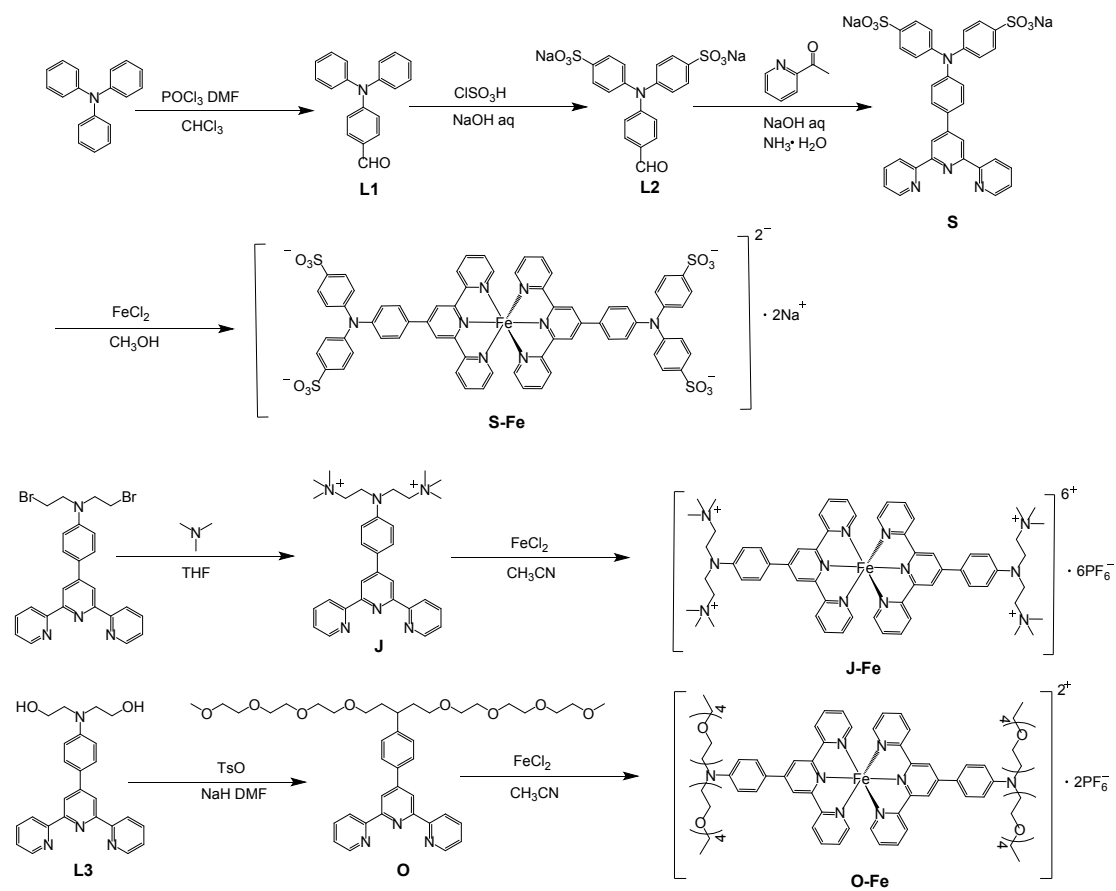
The cytotoxicity of **S-Fe**, **J-Fe** and **O-Fe** towards HeLa cells was determined by 5-dimethylthiazol-2-yl-2, 5-diphenyltetrazolium bromide (MTT) assay. The exponentially grown HeLa cells were seeded in triplicate into 96-well plates at  $10^4$  cells per well. After 48 h, the cells were treated with **S-Fe**, **J-Fe** and **O-Fe** respectively at different concentrations (100  $\mu$ M, 200  $\mu$ M, 300  $\mu$ M, 400  $\mu$ M, 500  $\mu$ M and 1000  $\mu$ M) and incubated for 24 h. After that time, the media was removed and the cells were rinsed once with PBS and placed with fresh media. Subsequently, cells were treated with 5 mg/mL MTT (10  $\mu$ L/well) and incubated for an additional 4 h (37 °C, 5% CO<sub>2</sub>). After MTT medium removal, the formazan crystals were dissolved in DMSO (100  $\mu$ L/well). The plate was incubated for 10 min while shaking it with an oscillator. The absorbance was measured at 450 nm using a microplate reader (SpectraMax Paradigm).

#### **PAI of S-Fe *in vivo***

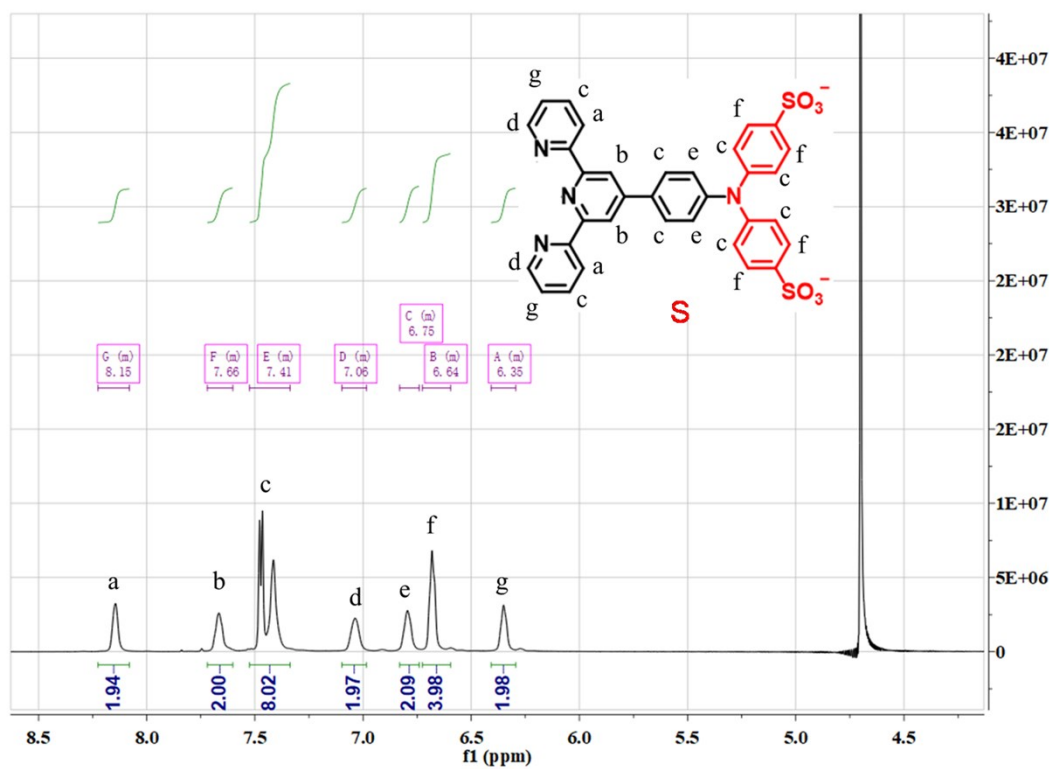
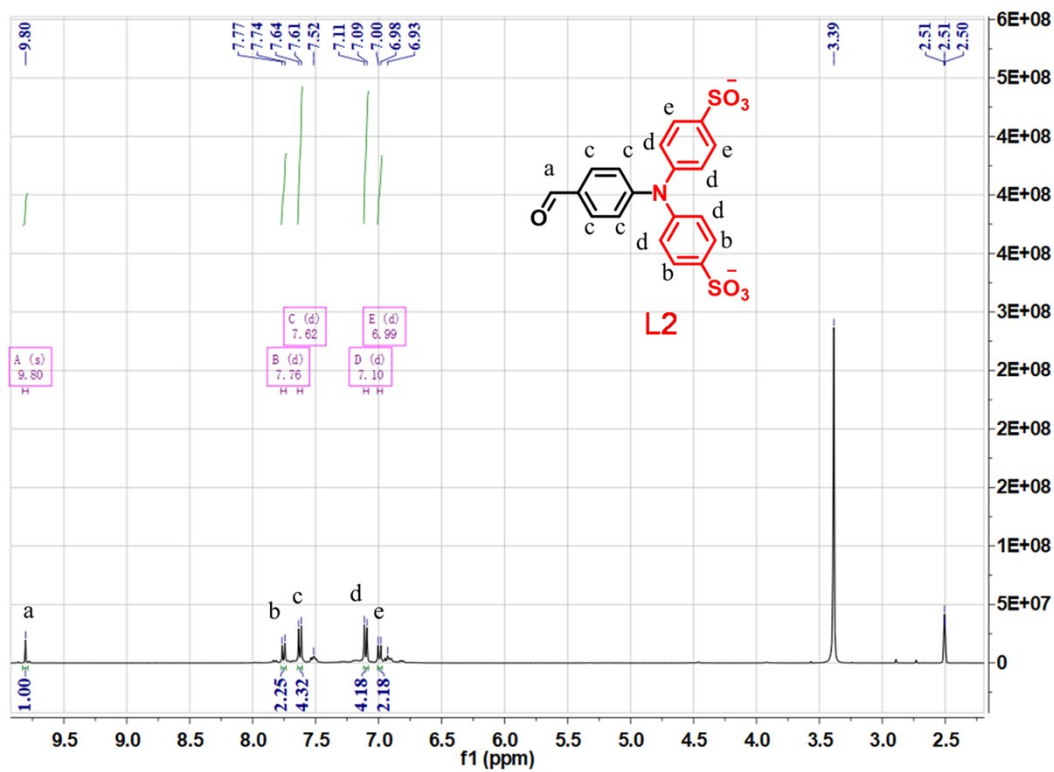
Injected **S-Fe** (200  $\mu$ L, 0.5 mM) into the tail of KuMing female mice (four-week size), intramuscular injection and intravenously injection, the signal intensity of liver, kidney and muscle were scanned every 15 min by photoacoustic imager. Two excitation wavelengths were

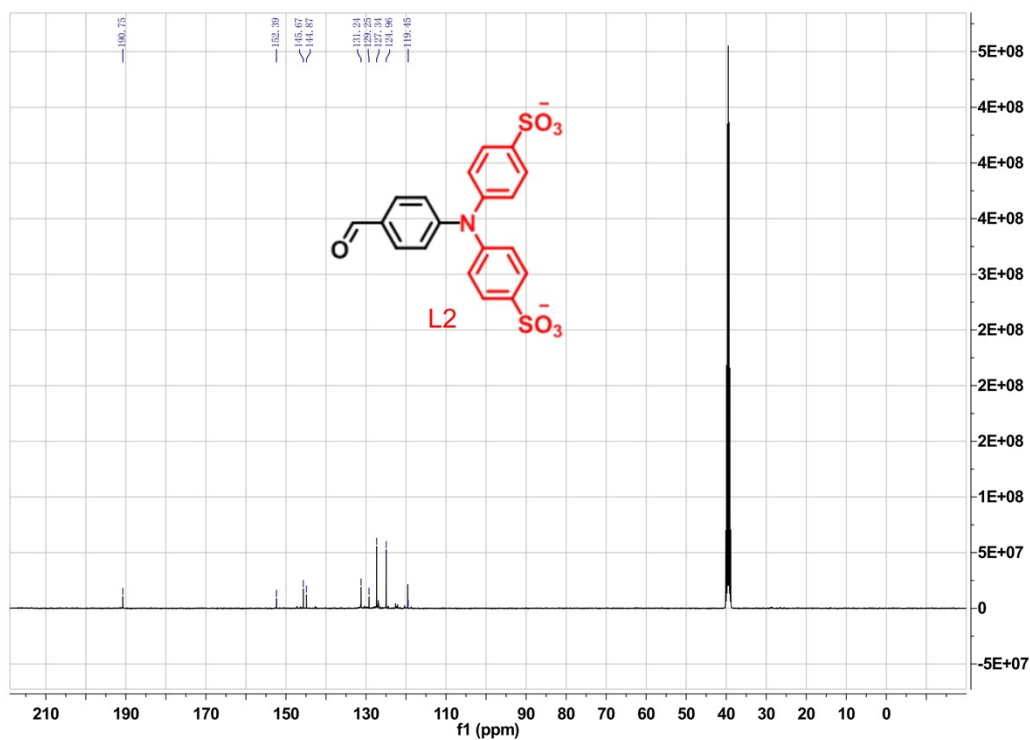
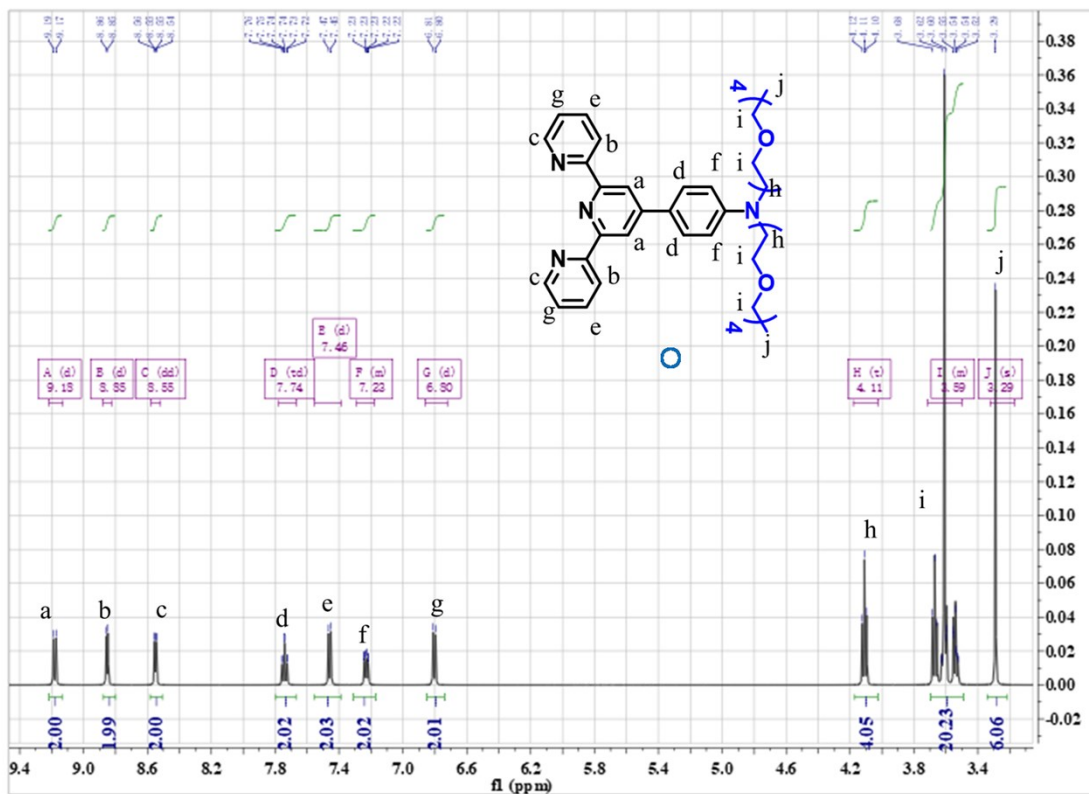
used to measure oxygenated and deoxygenated hemoglobin at 850 and 750 nm, respectively.

Photoacoustic signals before injection were recorded as controls (0 min).



**Scheme S1** Synthetic procedures for target molecules **S-Fe**, **J-Fe** and **O-Fe**.





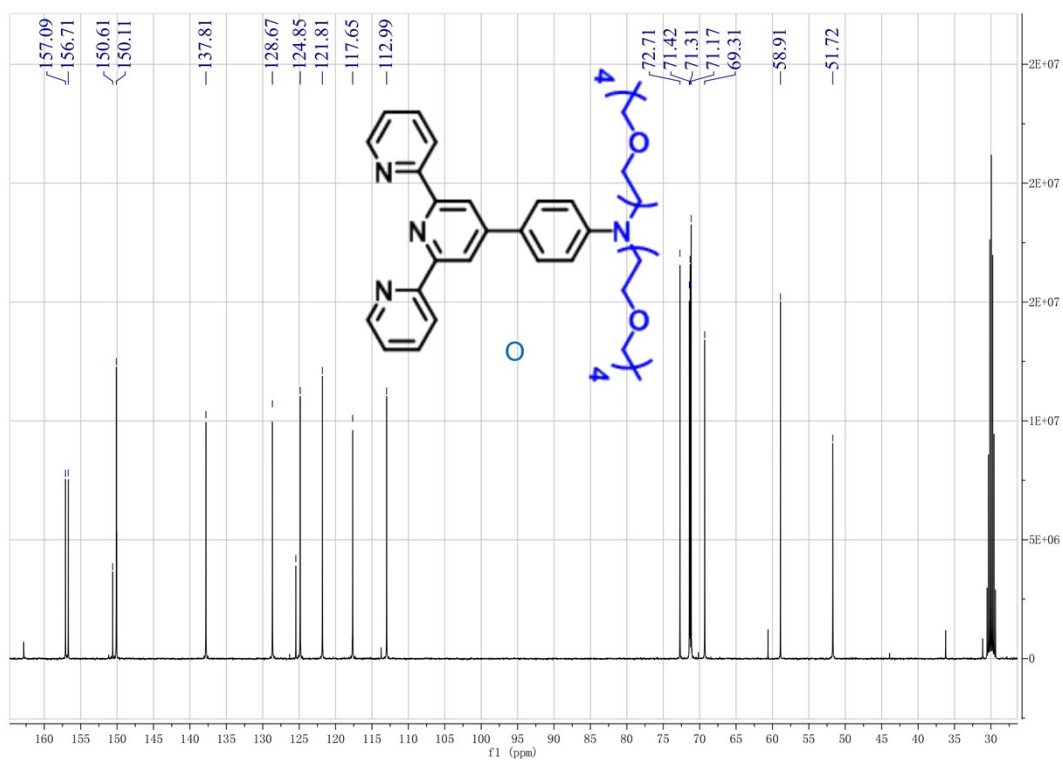
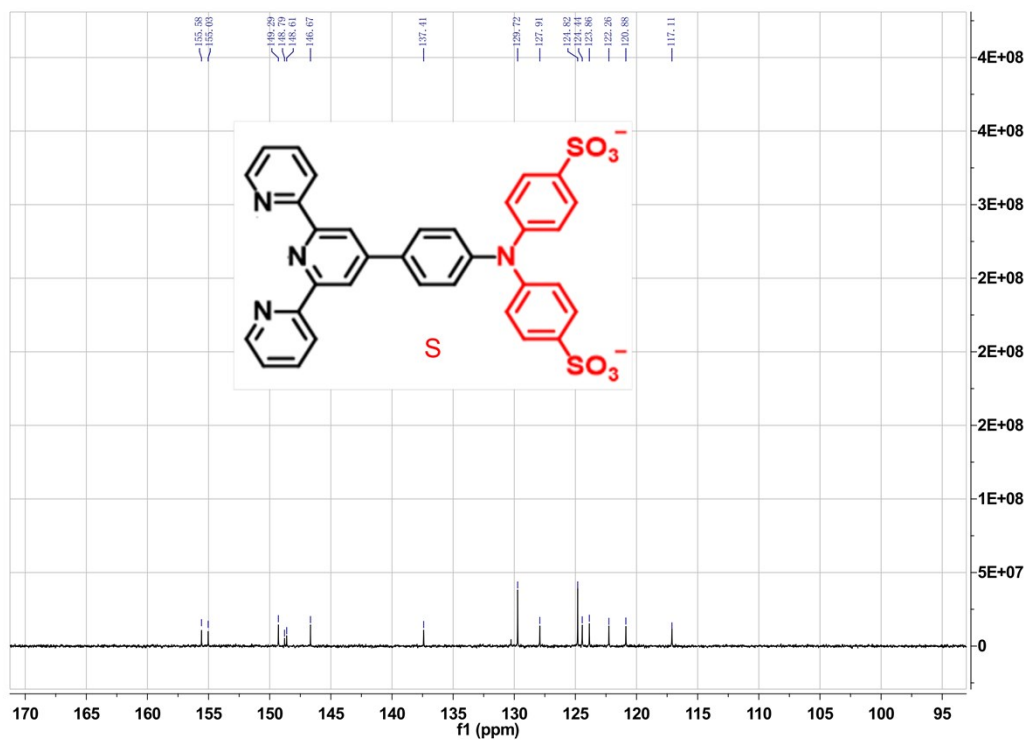
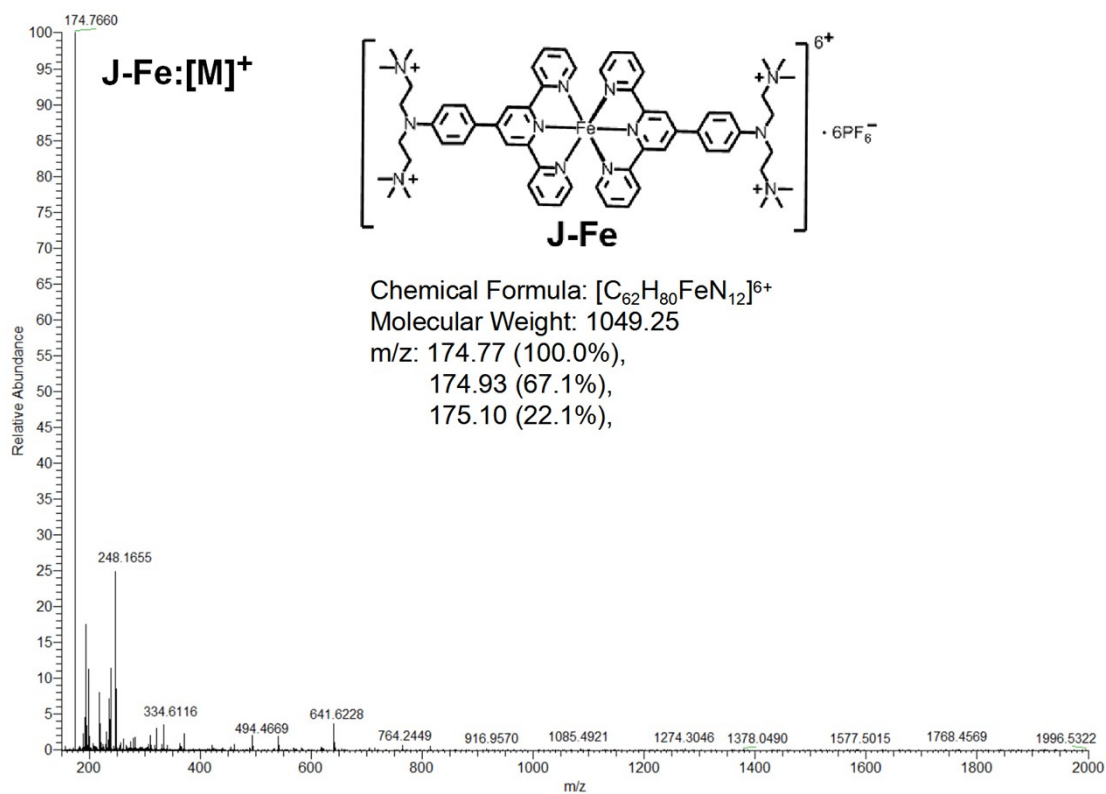
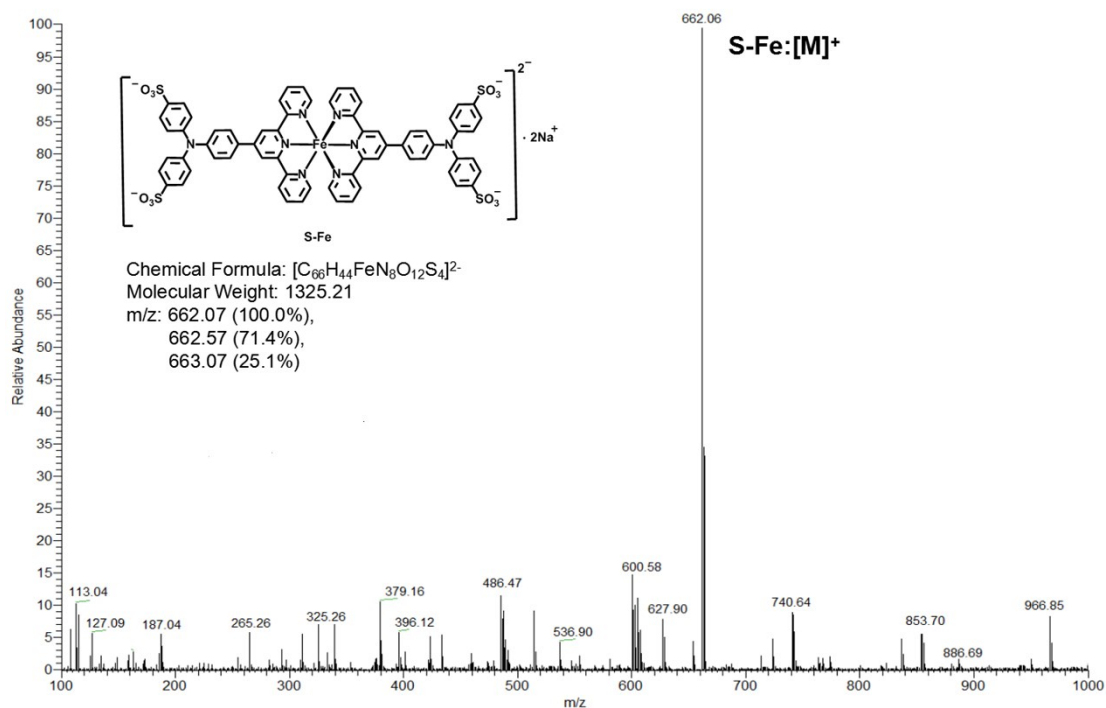
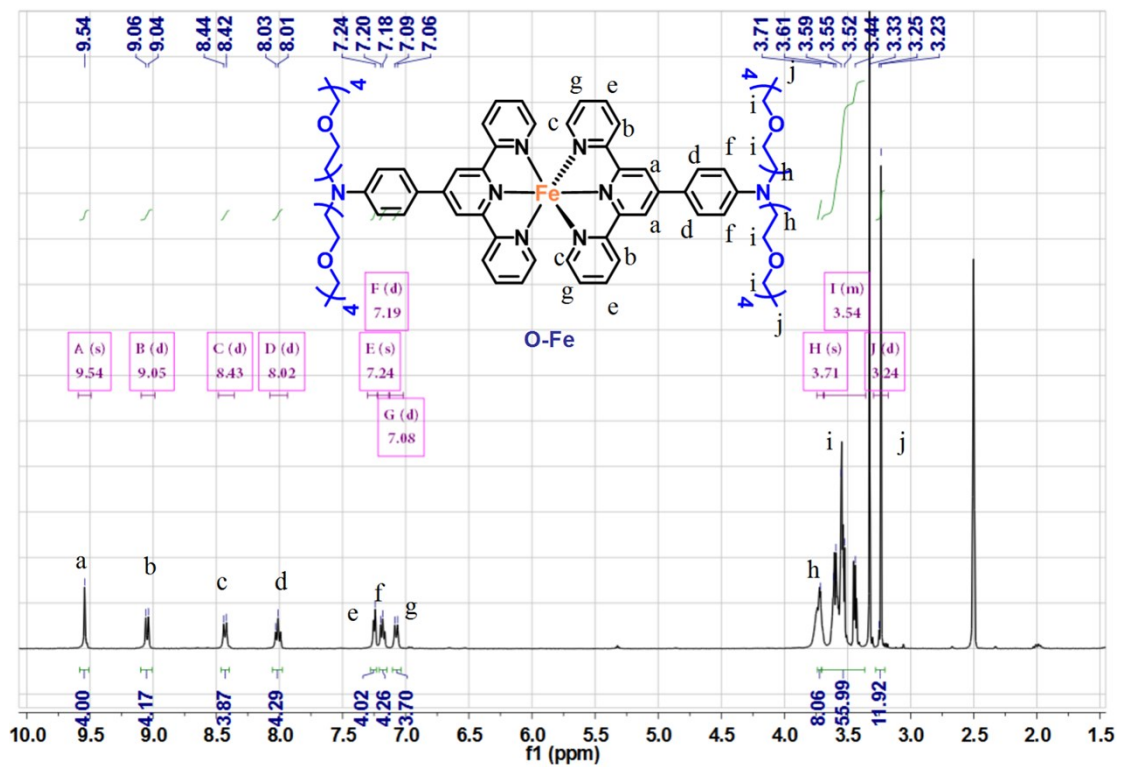
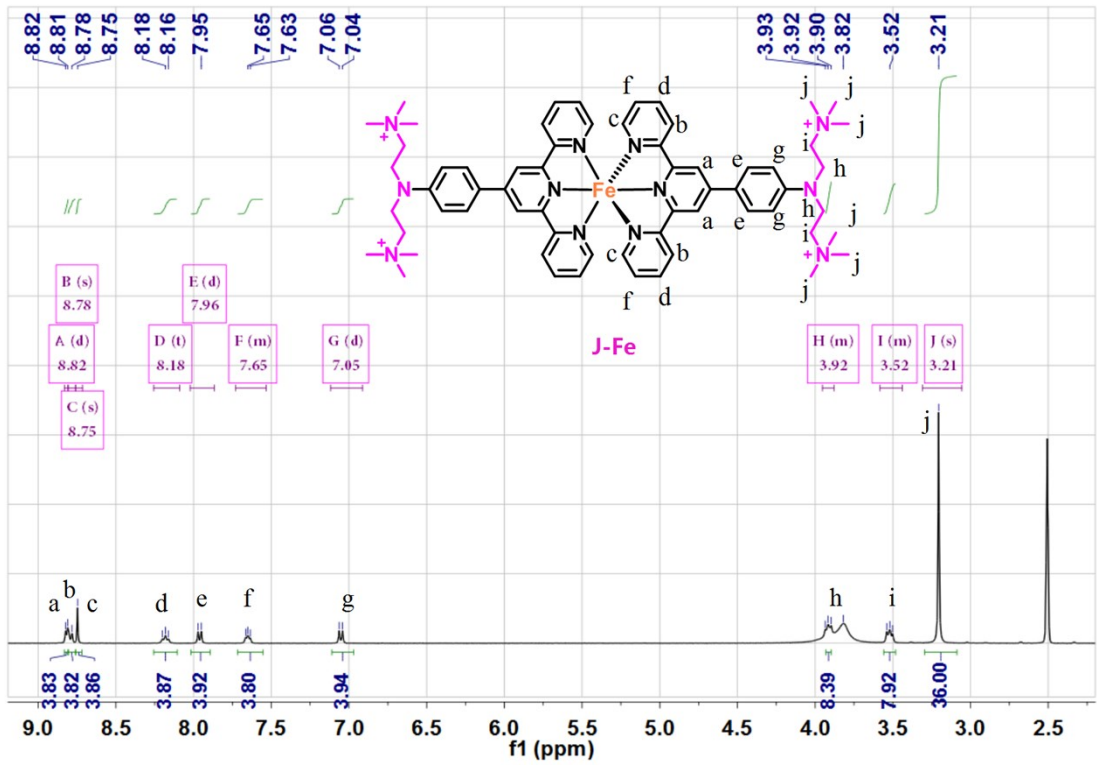


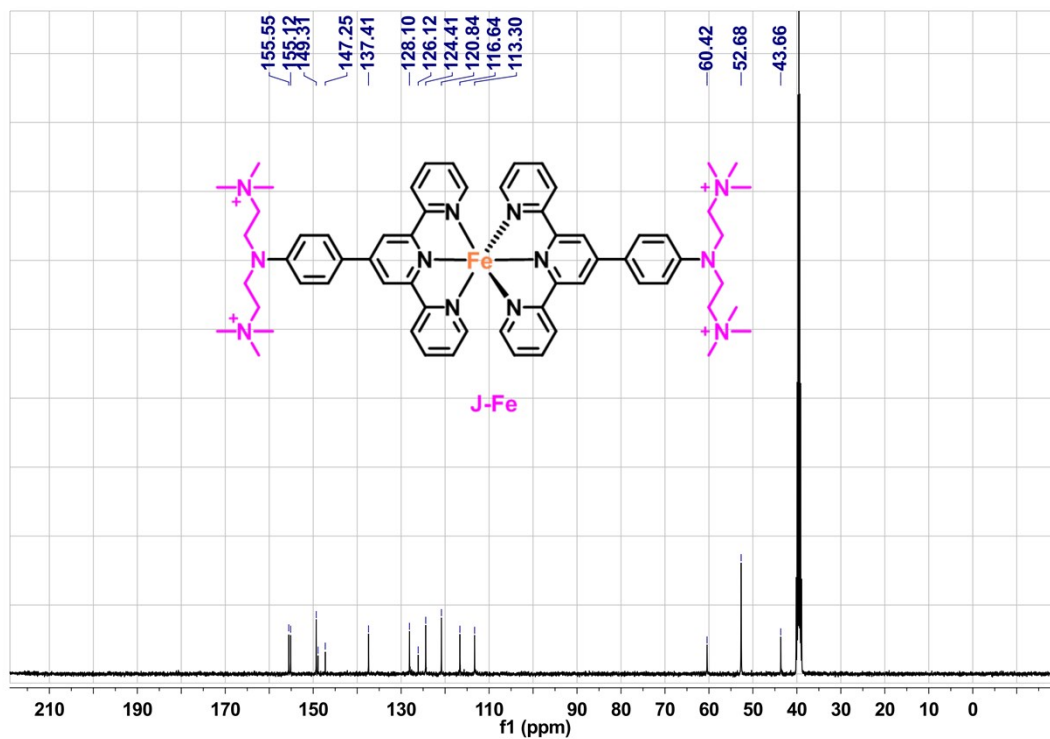
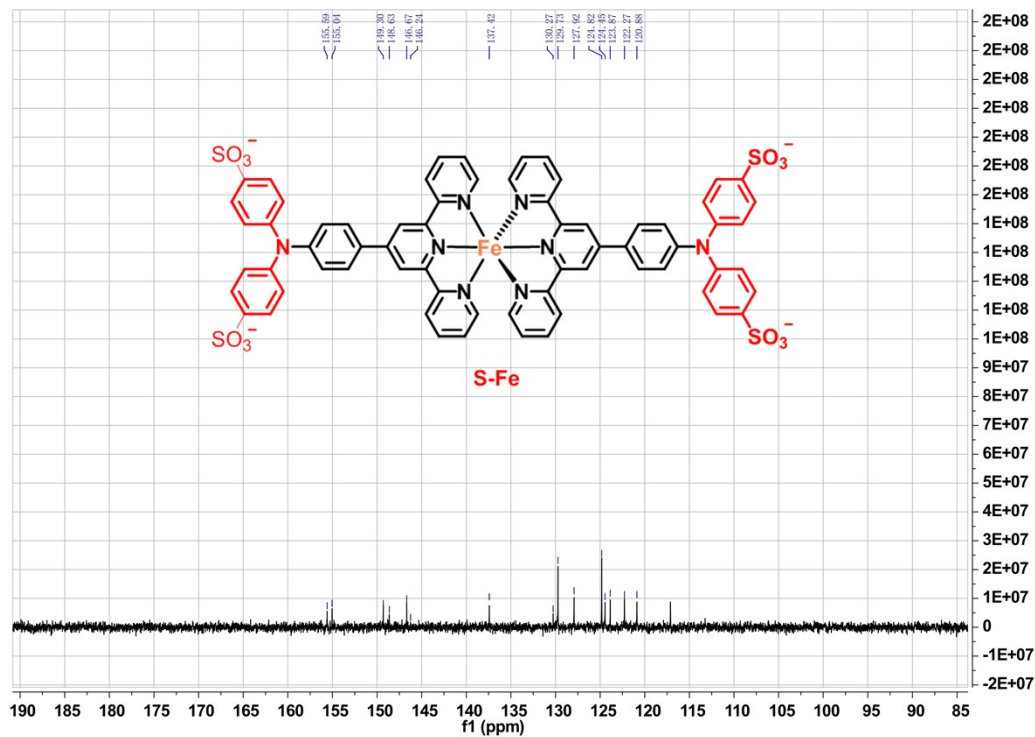
Figure S1.  $^1\text{H}$ -NMR and  $^{13}\text{C}$ -NMR spectra of L2, S and O.

T: fTMS + p ESI Full ms [100.00-1000.00]









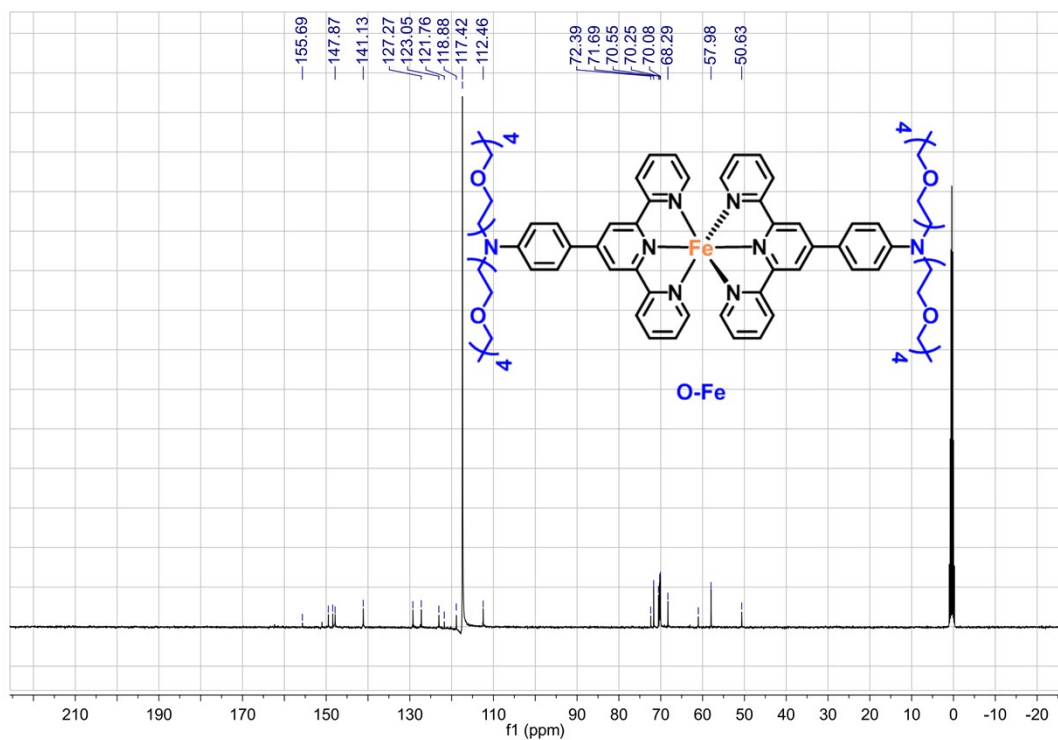


**Figure S2.** Mass spectra ,  $^1\text{H-NMR}$  and  $^{13}\text{C-NMR}$  spectra of S-Fe, J-Fe and O-Fe.

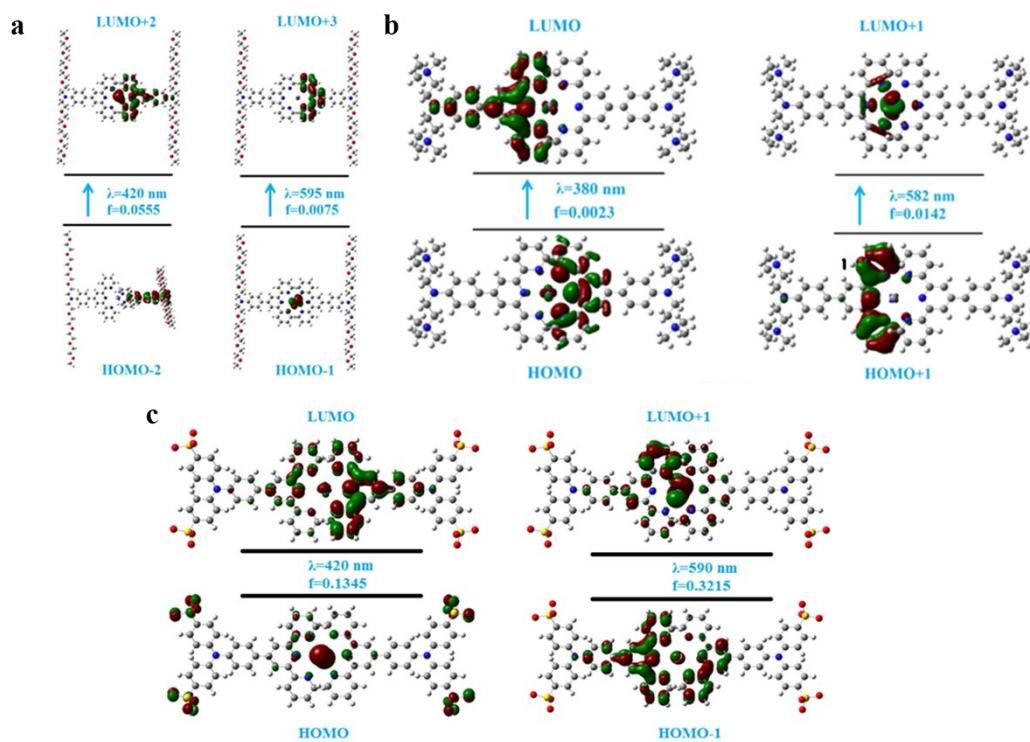


**Figure S3.** Molecular orbital energy diagrams of (a) O-Fe, (b) J-Fe and (c) S-Fe.

Sample	Absorbance (octanol)	Absorbance (ddH <sub>2</sub> O)	logP
S-Fe	0.299	0.001	-2.475671188
J-Fe	0.107	0.001	-2.029383778
O-Fe	/	/	/

**Figure S4.** Oil-water partition coefficient of S-Fe, J-Fe and O-Fe.

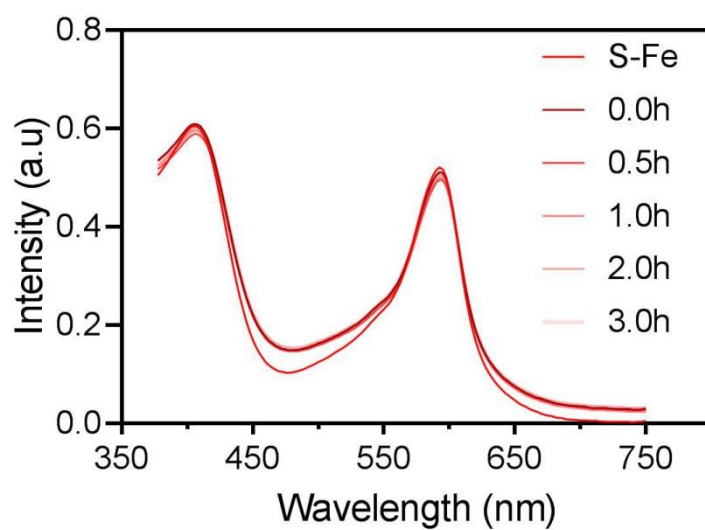


**Figure S5.** Ultraviolet absorption spectrum after incubation of S-Fe with 10% BSA.

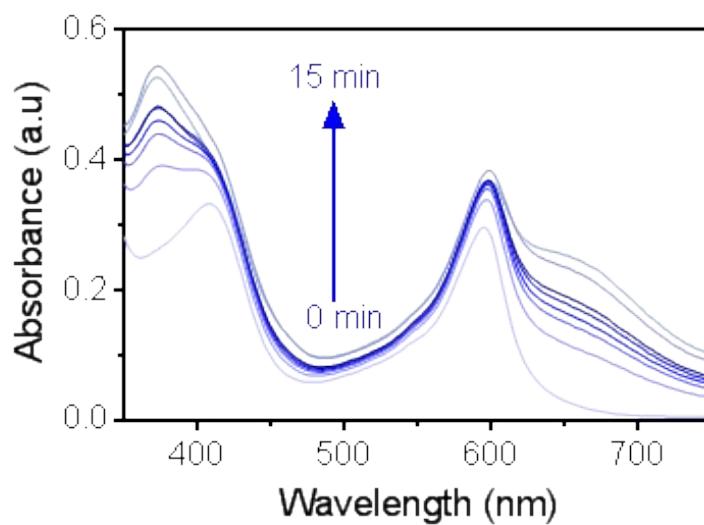


**Figure S6.** Rate of decay of TMB sensitized by S-Fe in PBS by the variation of the absorbance at 370 nm and 650 nm.

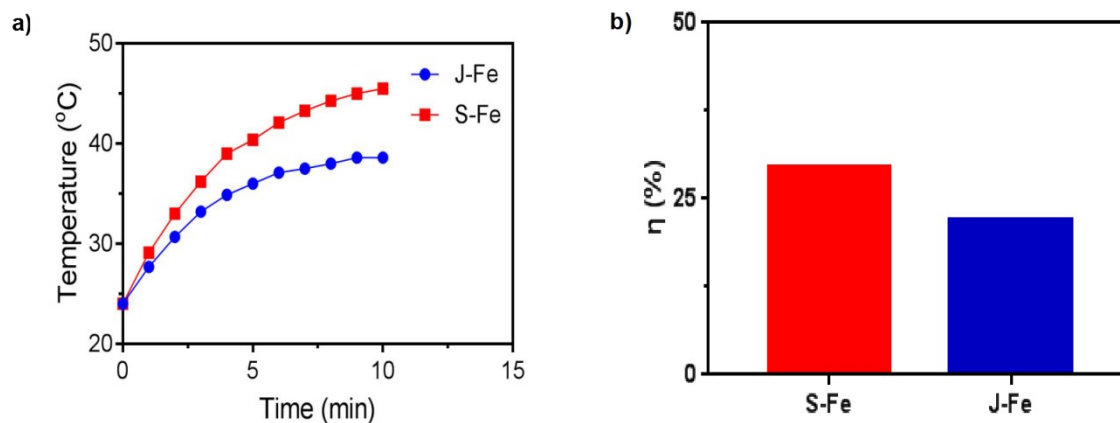


**Figure S7.** a) 808 nm laser irradiation (0.5, 1.0 and 1.5 W cm<sup>-2</sup>), heating curves of S-Fe and J-Fe aqueous solution. b) Photothermal conversion efficiency of S-Fe and J-Fe.

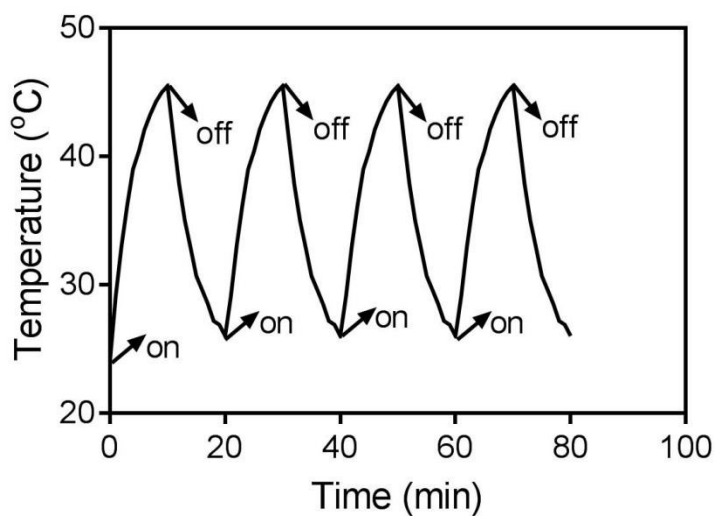


**Figure S8.** Thermal stability of S-Fe (four cycles of laser on/off) under 808 nm laser (1 W cm<sup>-2</sup>).

**Table 1.** Calculated linear absorption properties (nm), excitation energy (eV) and major contribution of S-Fe, J-Fe and O-Fe.

$\Delta E^{[a]}$	$\lambda^{[b]}$	Nature of the transition
------------------	-----------------	--------------------------

<b>O-Fe</b>	0.57	420	384(H-2)→389(L+2)	LMCT/LL'CT
	0.63	595	385(H-1) →390(L+3)	MLCT
<b>S-Fe</b>	0.57	420	336(H)→337(L)	MLCT
	0.63	595	335(H-1) →338(L+1)	LMCT
<b>J-Fe</b>	3.32	384	262(H)→263(L)	LL'CT
	2.12	582	261(H-1)→264(L+1)	LMCT

<sup>a</sup> The energy gap of the single-photon absorption band.

<sup>b</sup> Peak position of the maximum absorption band.

### Note and references

1. X. Tian, H. Wang, Q. Zhang, M. Zhang, Y. Zhu, Y. Chen, J. Wu and Y. Tian, *Analytica Chimica Acta*, 2018, **1008**, 82-89.
2. Q. Qiu, P. Xu, Y. Zhu, J. Yu, M. Wei, W. Xi, H. Feng, J. Chen and Z. Qian, *Chemistry – A European Journal*, 2019, **25**, 15983-15987.
3. C. Zhang, Y. Zhao, D. Li, J. Liu, H. Han, D. He, X. Tian, S. Li, J. Wu and Y. Tian, *Chemical Communications*, 2019, **55**, 1450-1453.
4. Z. Guo, W.-L. Tong and M. C. W. Chan, *Chemical Communications*, 2014, **50**, 1711-1714.
5. Y. Dong, Y. Sun, L. Wang, D. Wang, T. Zhou, Z. Yang, Z. Chen, Q. Wang, Q. Fan and D. Liu, 2014, **53**, 2607-2610.
6. W. Du, H. Wang, Y. Zhu, X. Tian, M. Zhang, Q. Zhang, S. C. De Souza, A. Wang, H. Zhou, Z. Zhang, J. Wu and Y. Tian, *ACS Applied Materials & Interfaces*, 2017, **9**, 31424-31432.
7. Z. Zheng, Q. Zhang, Z. Yu, M. Yang, H. Zhou, J. Wu and Y. Tian, *Journal of Materials Chemistry C*, 2013, **1**, 822-830.
8. M. Zerara, *Journal of Computational Chemistry*, 2008, **29**, 306-311.
9. C. Liu, S. Zhang, J. Li, J. Wei, K. Müllen and M. Yin, *Angewandte Chemie International Edition*, 2019, **58**, 1638-1642.